Available online at www.sciencedirect.com
SCIENCE DIRECT®
Journal of Sound and Vibration 281 (2005) 45–71
JOURNAL OF SOUND AND VIBRATION
www.elsevier.com/locate/jsvi

The role of damping on energy and power in vibrating systems

G. Pavic*

Laboratoire Vibrations – Acoustique, Institut National des Sciences Appliquees de Lyon, 20 Avenue Albert Einstein, 69621 Villeurbanne, France

Received 31 March 2003; accepted 7 January 2004

Abstract

The role of damping with respect to energy and energy flow in vibrating mechanical systems was examined with the aim of establishing some general relationships. The link between the energy flow and the system energy is considered from both the local and global points of view.

Locally, the mean intensity divergence is shown to be strictly proportional to the product of internal damping and potential energy density at a given point, while the imaginary value of complex divergence is proportional to the mean Lagrangian energy density. Globally, the mean value of the total vibratory power input to a structure is proportional to the volume integral of the product between the loss factor and the potential energy density. If the damping is uniformly distributed within a structure, this integral reduces to the product between the (constant) loss factor and the total potential energy.

The global potential and kinetic energies can be obtained from the known complex input power to the structure and the known loss factor. In the case of non-uniform damping, the simple power–energy relationships are shown to hold fairly well where potential energy is involved, but could break down if kinetic energy is used instead.

Several examples are given to illustrate the theoretical findings.

*Tel.: +33-4-72438707 fax: +33-4-72438712.
E-mail address: pavic@lva.insa-lyon.fr (G. Pavic).

0022-460X/$ - see front matter © 2004 Elsevier Ltd. All rights reserved.
doi:10.1016/j.jsv.2004.01.030

1. Introduction

The energy transmission in vibrating structures is a phenomenon the importance of which concerns both vibration theory and practice. The energy balance law universally applies to all forms of wave motions, vibratory and acoustic. Computational and measurement methods have been developed by means of which the energy flow in a vibrating structure can be traced. Most energy methods use a statistical notion of the global vibration field, e.g. [1–3]. Owing to its ostensible simplicity the Statistical Energy Analysis (SEA) has become the most used energy modelling concept. A particular value of SEA from the conceptual point of view is that it establishes a link between the stored energy and the energy flow.

Where the computation of energy in linear systems is concerned, modal superposition is the most commonly used approach in numerical analysis of vibration. The same approach can be used for the computation of energy flow as well. However, any precise computation of the latter will require summation over a large number of modes as the higher order modes with eigenfrequencies well above the excitation frequency will contribute decisively to energy flow. To overcome the modal computation problem a hybrid technique has been proposed in which the contribution of higher modes is accounted for via an independently computed static solution [4].

Classical SEA refers to the stored energy as 'energy', the energy being the total mechanical energy of the system concerned, i.e. the sum of kinetic and potential energies. In SEA applications it is tacitly assumed that the two constituent energies are equal. The practical importance of this assumption lies in the possibility to express the stored energy in terms of kinetic energy, the one which is much easier to handle. While in systems of high modal density the two energies are indeed practically identical in the global sense, their spatial distributions—the kinetic and potential energy densities—are not. Moreover, the total energy density, i.e. the sum of the two, is not uniformly distributed across a vibrating structure which hinders the use of global concepts, such as SEA, at the local level. Attempts to establish an SEA equivalent based on local energy variables, see e.g. Refs. [5–8], have not yielded results comparable to the original, lumped parameter SEA. In [9] Carcaterra and Sestieri have shown that the construction of comprehensive differential energy equations leading to vibrational-thermal analogy may be out of reach where a general case is concerned.

Back to the deterministic approach, the literature on energy distribution and energy flow in structures is sparse. A rather detailed study on this topic with application to elastic waves in solids was made by Maysenhölder [10]. Some useful notions of energy flow and energy density in solid waves can be found in Chapter 5 "Power flow and energy balance" of a textbook by Auld [11]. A similar subject was addressed in a paper by Alfredsson, [12]. However the practical applicability of these "exact" approaches is not as wide as is that of statistical ones. The exception is the measurement of energy flow which has received some considerable attention. It is worth noting that, while various techniques have been developed on the topic of energy flow, the measurement of energy in structures was fairly neglected. In particular, measurement of potential energy was never considered as an issue.

This paper concerns the role of structural damping on energy and energy flow. An explicit formulation of the relationship between these two quantities will be shown and demonstrated over several examples.

2. Global energy and energy flow

In this paper sinusoidal time variation of primary quantities, forces and velocities, will be assumed. The sinusoidal form of time variations enables use of complex representation of these quantities. All the quadratic quantities, such as energy or power, resulting from the multiplication of primary ones, will be taken as time averaged. The averaged product of two sinusoidally varying quantities represented in complex form reduces to the real part of the product of their complex amplitudes:

$$\overline{u_1(t)u_2(t)} \hat{=} \frac{1}{2}\mathrm{Re}\left\{U_1 U_2^*\right\} \quad {}^* - \text{complex conjugate.}$$

Energy will be considered as a purely real quantity while the time-averaged values of power and intensity will be considered as complex quantities. Thus in referring to the time-averaged power or intensity a substitute complex quantity will be employed, the real part of which equals the physical quantity itself. The imaginary part of such a complex quantity, in spite of missing a clear physical meaning, will be employed too as this part provides some extra information useful for the analysis.

In sinusoidal vibration the relationship between the net (real) input power P and the global energy E is usually expressed by an approximation, see e.g. [1]:

$$\bar{P} \approx \eta\omega\bar{E} \tag{1}$$

where $\bar{}$ denotes time average, ω denotes frequency and η denotes system damping. The symbol E stands for the total mechanical energy, i.e. the sum of potential and kinetic energies, $E = E_p + E_k$.

Eq. (1) is often used in statistical analysis where an extra averaging in addition to time averaging, over a frequency band, is applied. It can be further simplified by assuming equality between the time averaged kinetic and potential energies:

$$\bar{E}_k \approx \bar{E}_p \Rightarrow \bar{P} \approx 2\eta\omega\bar{E}_k \tag{1a}$$

The relationships between global variables, Eqs. (1) and (1a), will be examined in this section with the view of finding the origin of these outside the scope of statistical framework. To this end a modal series solution will be used to represent a vibration field.

Consider a linear system excited by multiple forces. The usual expansion of vibration displacement in normalized natural functions ϕ_q, $q = 1,2,\ldots$, will be made (time factor $e^{j\omega t}$ omitted) [13]:

$$u(x,\omega) = \sum_q U_q(\omega)\phi_q(x), \quad U_q(\omega) = \frac{1}{m}\frac{f_q}{\Omega_q} \tag{2a}$$

with

$$f_q = \sum_n F_n(\omega)\phi_q(z_n), \quad \Omega_q = \omega_q^2\left(1 + j\eta_q\right) - \omega^2 \tag{2b}$$

where x is the coordinate of a response point, U_q the modal amplitude (complex), m the total mass, ω_q the natural frequency, f_q the modal force (complex) and Ω_q the modal frequency factor (complex). The external excitation is taken as a superposition of forces F_n acting at positions z_n, $n = 1, 2, \ldots$.

Assuming orthogonality, the overall time-averaged kinetic energy and total net input power can be expressed in terms of single modal summation, Appendix A:

$$\bar{E}_k = \frac{m\omega^2}{4}\sum_q |U_q|^2, \quad \bar{P} = \frac{m\omega}{2}\sum_q \eta_q \omega_q^2 |U_q|^2. \tag{3}$$

If a single mode dominates close to its resonant frequency, the simple formula (1b) for kinetic energy becomes valid

$$\omega \to \omega_q \Rightarrow \bar{E}_k \approx \frac{1}{4m}\frac{|f_q|^2}{\eta_q^2\omega^2}, \quad \bar{P} \approx \frac{1}{2m}\frac{|f_q|^2}{\eta_q\omega} \Rightarrow \bar{P} \approx 2\eta\omega\bar{E}_k. \tag{3a}$$

Eq. (3a) is given in terms of kinetic energy only. General form of potential energy cannot be assessed by modal approach the same way as that of kinetic energy, Eq. (3), because the potential energy depends on the particular characteristics of the system considered.

The kinetic and potential energies are almost equal at resonance, but not at other frequencies. Below the resonance potential energy of a particular mode is larger than kinetic, while the opposite applies above the resonance. In the case of high modal overlap, at any particular excitation frequency, the (lower) kinetic energy of modes having the eigenvalues above the excitation frequency will become compensated by the (higher) kinetic energy of lower modes. Inverse compensation effect will apply to potential energy. As a result, the global kinetic and potential energies in modally overlapped systems can be shown to match closely at all frequencies except below the first resonance where the compensation cannot take place. This justifies approximation (1a).

Since both the system energy and input power can be reduced to a single modal summation, the terms under the summation sign represent modal kinetic energy $e_{k,q}$ and modal power p_q:

$$e_{k,q} = \frac{m\omega^2}{4}|U_q|^2 \Rightarrow \bar{E}_k = \sum_q e_{k,q}, \tag{4a}$$

$$p_q = \frac{m\omega}{2}\eta_q\omega_q^2|U_q|^2 \Rightarrow \bar{P} = \sum_q p_q. \tag{4b}$$

The relationship between the energy and power can now be brought to the modal level:

$$p_q = 2\omega\eta_q\left(\frac{\omega_q}{\omega}\right)^2 e_{k,q}. \tag{5}$$

The modal relationship has the same form as the approximate global relationship (1a) except for the factor equal to the ratio square of eigenfrequency and excitation frequency. This factor explains the nature of power–energy relationship with respect to frequency: below a resonance the kinetic energy is overestimated by the input power, while above a resonance it is underestimated.

The potential energy of a single-degree-of-freedom (dof) system is related to its kinetic energy via the same frequency ratio factor as appearing in Eq. (5)

$$E_p = E_k\left(\frac{\omega_{\text{res}}}{\omega}\right)^2, \tag{6}$$

where ω_{res} is the resonant frequency. Since any multi-dof system can be represented as a canonical circuit of a series of single-dof systems, [13], it could be argued that the modal relationship between the potential energy and input power can be obtained by inserting Eq. (6) into Eq. (5) to yield

$$p_q = 2\omega\eta_q e_{p,q}. \tag{4c}$$

As a matter of fact, Eq. (4c) is valid for any system with N degrees of freedom. This in turn gives

$$\bar{P} = 2\eta\omega\bar{E}_p. \tag{7}$$

The last equation is free from the frequency weighted factor appearing in Eq. (5). It will hold exactly, as long as the loss factor is the same for all modes. An alternative validation of this central relationship will be provided in Section 3 using a non-modal approach.

Eqs. (1) and (3) are valid for the whole structure exhibiting resonant behaviour. These cannot be applied at the local level, i.e. for an analysis of energy distribution within a structure.

The modal character of the local energy distribution can be examined only in some general way, see Appendix A. At a given response point the unit energy flow, the intensity, can be represented in modal terms as a double sum of a series, Eq. (A.8). It has been shown that different modes and different excitations (if more excitations exist than a single one) interact in the local distribution of energy flow. The energy flow will exist even if there is no dissipation, i.e. $\eta = 0$, providing that more than one excitation acts on the body.

2.1. Example 1: energy and input power of a rectangular plate

To examine the validity of expressions (3a) and (7) which relate the kinetic and potential energy to the input power, flexural vibration of a rectangular plate made of plexiglass will be analysed. The plate is taken simply supported along two shorter edges and simply guided along the remaining edges, Fig. 1. The plate parameters are: Young's modulus $E = 4.95\,\text{GPa}$, mass density $\rho = 1150\,\text{kg/m}^3$, Poisson's ratio $\upsilon = 0.305$, loss factor linearly increasing with frequency between $\eta = 1\%$ at 0 Hz and 3% at 1kHz, thickness $h = 20\,\text{mm}$, length $a = 0.5\,\text{m}$, width $b = 0.35\,\text{m}$.

The plate is assumed to be driven by a force acting across a massless lever of length $d = 10\,\text{cm}$ oriented at an angle $\alpha = 45^\circ$ with respect to the longer edge. In this way the excitation transmitted to the plate consists of a normal force and a bending moment acting at the same point. To make

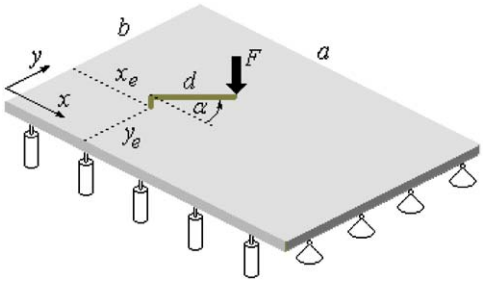

Fig. 1. Model of a rectangular plate

the computation simple, the plate is aligned with the x–y Cartesian system. The excitation position has been arbitrarily picked out at: $x_e = 0.155\,\mathrm{m}$, $y_e = 0.143\,\mathrm{m}$ relative to one of the corners.

The choice of non-homogeneous boundaries, dual-type excitation and variable damping was made simply to distract the reader from the omnipresent simply supported, constant damping, pure force excitation case.

Under the chosen boundary conditions:

$$x = 0 \text{ and } x = a: \quad x = 0 \text{ and } \partial^2 u/\partial x^2 = 0,$$
$$y = 0 \text{ and } y = b: \quad \partial u/\partial y = 0 \text{ and } \partial^3 u/\partial y^3 = 0$$

the eigenvalues and the normalized eigenfunctions can be readily evaluated

$$\omega_{q'q''} = \sqrt{\frac{B'}{m''}}\pi^2\left[\left(\frac{q'}{a}\right)^2 + \left(\frac{q''}{b}\right)^2\right], \quad \phi_{q'q''} = \delta\ \sin\left(\frac{q'\pi x}{a}\right)\cos\left(\frac{q''\pi y}{b}\right),$$
$$q' = 1, 2, 3..., \quad q'' = 0, 1, 2, 3...$$

with B' and m'' the flexural stiffness and unit surface mass while $\delta = 2^{[1+\mathrm{sign}(q'')]/2}$. The modal excitation comprising the force and moment loading will be in this case

$$f_{q'q''} = F\phi_{q'q''} + Fd\cos(\alpha)\frac{\partial\phi_{q'q''}}{\partial x} + Fd\ \sin(\alpha)\frac{\partial\phi_{q'q''}}{\partial y}$$
$$= 2F\left\{\sin(\kappa_x)\cos(\kappa_y) + d\pi\left[\frac{q'}{a}\cos(\alpha)\cos(\kappa_x)\cos(\kappa_y) - \frac{q''}{b}\cos(\alpha)\sin(\kappa_x)\sin(\kappa_y)\right]\right\},$$
$$\kappa_x = \frac{q'\pi x_e}{a}, \quad \kappa_y = \frac{q''\pi y_e}{b}, \quad q' = 1, 2, 3..., \ q'' = 0, 1, 2, 3...,$$

where the term in square brackets is due to moment loading of the plate Fd split into two orthogonal components. With the eigenvalues and modal excitations identified, the modal displacement amplitude $U_{q'q''}$ defined by Eq. (2a) becomes fully known.

The unit-surface potential energy of a flat plate reads [14]

$$E_p'' = \tfrac{1}{2}B\left[\left(\frac{\partial^2 u}{\partial x^2}\right)^2 + \left(\frac{\partial^2 u}{\partial y^2}\right)^2 + 2\upsilon\frac{\partial^2 u}{\partial x^2}\frac{\partial^2 u}{\partial y^2} + 2(1-\upsilon)\left(\frac{\partial^2 u}{\partial x \partial y}\right)^2\right].$$

By expanding in modal series using the defined eigenfunctions and integrating across the plate area with the aid of orthogonality, the modal components of potential energy are found to be equal to

$$e_{p,q'q''} = \frac{B}{4}\pi^4\left[\left(\frac{q'}{a}\right)^2 + \left(\frac{q''}{b}\right)^2\right]^2\left|U_{q'q''}^2\right| = \frac{m}{4}\omega_{q'q''}^2\left|U_{q'q''}^2\right|.$$

The expression (4a) predicting the relationship between the modal kinetic energy and the modal net input power is thus proved in this case. The modal net power is given by Eq. (4b).

Fig. 2 shows the global energy in plate (a) and the net input power (b) under a 100 N force excitation. The energy plot shows the total energy (i.e. the sum of kinetic and potential energies) as well as the Lagrangian energy (i.e. the difference of the two). Showing the total and Lagrangian

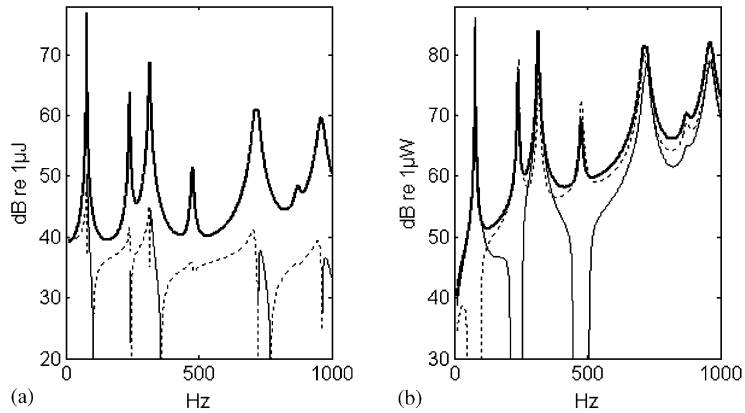

Fig. 2. (a) Energy of a flat plate. Thick line: total energy, thin line: positive values of Lagrangian energy, dashed line: negative values of Lagrangian energy. (b) Power in a flat plate. Thick line: net input power, thin line: positive values of force-supplied net input power, dashed line: positive values of moment-supplied net input power.

energy rather than kinetic and potential energy improves visibility because the latter two overlap a lot and are not easily identifiable on a common logarithmic plot except at low frequencies where the kinetic energy rapidly drops with frequency toward zero.

The Lagrangian energy can be seen to be mostly negative (thin dotted line); only at short frequency intervals closely following the well-isolated resonant frequencies the kinetic energy exceeds the potential energy. The relative difference of the two energies is the largest between the resonances.

As there are two mechanisms of power input, force and moment, the total input power will be the sum of the two. While its net value is identically positive, one of its components—force-supplied or moment-supplied one—may get negative at some frequencies. E.g. the negative moment-supplied power means that the force is injecting only one part of its power into the plate, the other part being taken away by the moment. Plot (b) represents the total input power (thick line) along with the positive values of its force-supplied (thin full line) and moment-supplied (thin dashed line) components. A closer look shows that at frequencies ~50 to 100 Hz the moment drains some power away, while the same applies to the force at ~205 to 260 Hz and ~450 to 500 Hz.The net input power will nevertheless stay proportional to the global potential energy at all frequencies in accordance with Eq. (7).

Fig. 3 indicates the limitations of the use of simplified relationships between energy and energy flow. Plot (a) shows the loss factor estimate from the known input power and known global energy. The other plot shows the relative error in the loss factor estimate for 3 different values of damping: the reference damping 1% (bold line), 0.1% (thin line) and 10% (dashed line).

Both estimates can be seen to give large errors at frequencies between resonances. At resonances the matching between the estimated and exact values are good. The amount of damping does not affect much the accuracy of estimation except at high frequencies where larger damping produces larger estimation error.

The evaluation of loss factor using the potential energy formulation, Eq. (7), yields its exact value as expected.

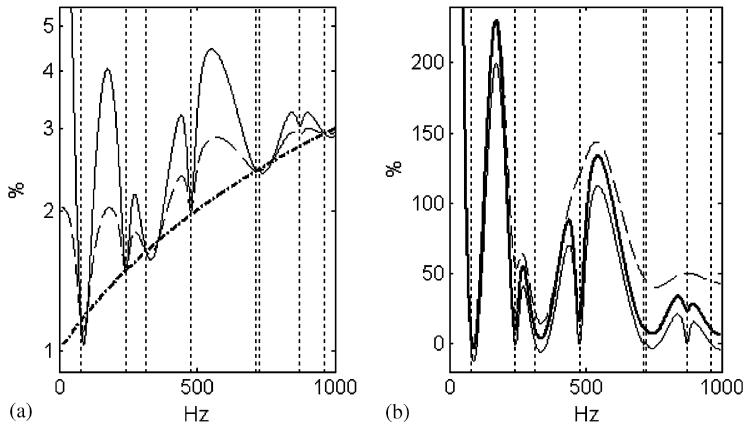

Fig. 3. (a) Estimate of loss factor in a flat plate via kinetic energy, Eq. (1a) (thin line) and total energy, Eq. (1) (dashed line). Bold dash-dot line is the exact value of loss factor. (b) Error of estimate via kinetic energy at different values of mean damping: thin line: 0.2%, thick line: 2%, dashed line: 20%. Vertical lines represent positions of resonant frequencies.

3. Local distribution of energy and energy flow within a structure

Energy flow balance for an elementary volume of an elastic lossless solid free from volume forces is given by Poynting theorem applied to elastic solids [11]

$$\frac{\partial e}{\partial t} + \mathrm{div}(\mathbf{I}) = 0, \tag{8}$$

where t stands for time, e for energy density, $\mathbf{I}$ for intensity vector.

Eq. (1) applies to instantaneous values. In a steady-state motion the time-averaged energy variation is zero. The mean intensity divergence thus vanishes at each point

$$\overline{\partial e/\partial t} = 0 \Rightarrow \mathrm{div}(\mathbf{I}) = 0.$$

In order to make formula (8) applicable to a dissipative solid, a term has to be added equal to the temporal rate of change of dissipated energy within the elementary volume. In steady-state motion, the energy density dissipated in unit time thus becomes equal to the negative value of intensity divergence.

The relationship between the dissipated energy density and intensity divergence, while providing clear physical justification of the energy loss balance, is of little practical value when it comes to the relationships between energy density and energy flow (intensity).

Several authors have shown that the following equalities regarding the complex input power $\bar{P}_{\mathrm{in}}$ were rigorously satisfied for a linear solid medium, [11,12,15]

$$\mathrm{Re}(\bar{P}_{\mathrm{in}}) = P_{\mathrm{diss}}, \tag{9a}$$

$$\mathrm{Im}(\bar{P}_{\mathrm{in}}) = 2\omega(\bar{E}_p - \bar{E}_k) \tag{9b}$$

with the symbols Re and Im denoting real and imaginary parts, respectively.

Some useful relationships between energy variables of a multi-point driven vibrating system were set up by Bobrovnitskii [16]. These involve the driving point impedance $Z(\omega)$:

$$P_{\text{diss}} = \tfrac{1}{2}\text{Re}(Z)\left|V^2\right|, \tag{10a}$$

$$\bar{E}_p - \bar{E}_k = \tfrac{1}{4}\text{Im}\left(\frac{Z}{\omega}\right)\left|V^2\right|, \quad \bar{E}_p + \bar{E}_k \approx \tfrac{1}{4}\text{Im}\left(\frac{\partial V}{\partial \omega}\right)\left|V^2\right|. \tag{10b}$$

Expressions (9a) and (10a) involving the dissipated power P_{diss} are self-obvious as these follow from some basic energy balance. The remaining expressions involving energies are less obvious. These expressions represent a valuable tool in the assessment of global properties of vibrating structures. It can be seen that the equation for energy difference in Eq. (10b) corresponds to Eq. (9b). It is strictly valid. The equation for energy sum in Eq. (10b) is only an approximation. It is strictly valid only for a system with no losses.

The limitation of Eq. (10a,b) is in the nature of excitation (single point). Besides, the expression for the sum of energies is approximate only, not applicable to all frequencies. In a later paper the same author has improved the approximation but the limitation to a single input remains [17].

3.1. Explicit formulation of energy density and intensity (fundamental relationship)

A basic relationship is established in Appendix B, linking the energy density and energy flow in an elastic damped structure, Eqs. (B.16) and (B.17). The kinetic and potential energy densities are evaluated explicitly, not only in terms of their difference. The analysis is made using an engineer's rather than a physicist's approach which was judged to be more appropriate to the readers. Thus classical expressions for displacements, stresses and strains were employed instead of more condensed tensorial ones which comprise summation conventions. While the expressions for an isotropic and homogeneous medium were used throughout, the results are valid for any linear medium providing the damping stays isotropic. The loss factor can have arbitrary frequency dependence but has to comply with the concept of complex elasticity modulus.

To start with, the notion of complex energy flow is introduced. The density of energy flow, i.e. the intensity, is given as a linear combination of products between stresses and velocities, (B.6). Under the complex notation used to represent sinusoidal time variations these (real) products are transformed into complex products between stress amplitudes and conjugate velocity amplitudes. The real part of complex energy flow corresponds exactly to the temporal mean value of true energy flow, i.e. to the net energy flow.

The divergence of complex intensity vector $\mathbf{I}$ and the kinetic and potential energy densities, e_p and e_k, were shown to satisfy the following equation:

$$\nabla \cdot \mathbf{I} = \text{Re}(\nabla \cdot \mathbf{I}) + \text{jIm}(\nabla \cdot \mathbf{I}) = 2\omega\left[\bar{e}_p(\text{j} - \eta) - \text{j}\bar{e}_k\right]. \tag{11}$$

In evaluation Eq. (11) the loss factor was accounted for via a complex elasticity modulus as defined by Cremer et al, [18]. Eq. (11) is thus very general as any damping in a linear, sinusoidally vibrating system can be represented by an appropriate complex elasticity modulus [13]. It has been assumed that the loss factors relative to compression and shear moduli are identical, equal to η in Eq. (11). Such isotropy of damping is indispensable if Eq. (11) is to stay simple.

Assume the loss factor η be constant across the whole vibrating object. By integrating over the body volume and applying the Gauss–Ostrogradsky formula the following result is obtained:

$$\bar{P}_{\text{in}} = -\int_S \mathbf{I}\cdot\mathbf{n}\,\mathrm{d}S = -\int_V \operatorname{div}(\mathbf{I})\,\mathrm{d}V = 2\omega\left[\mathrm{j}\bar{E}_k + (\eta - \mathrm{j})\bar{E}_p\right]. \tag{12}$$

Thus kinetic and potential energies of the vibrating body can be expressed as simple functions of total complex mechanical power supplied:

$$\bar{E}_p = \frac{\operatorname{Re}(\bar{P}_{\text{in}})}{2\eta\omega}, \tag{12a}$$

$$\bar{E}_k = \frac{\operatorname{Re}(\bar{P}_{\text{in}}) + \eta\operatorname{Im}(\bar{P}_{\text{in}})}{2\eta\omega} \approx \frac{\operatorname{Re}(\bar{P}_{\text{in}}\mathrm{e}^{-\mathrm{j}\eta})}{2\eta\omega}, \tag{12b}$$

$$\bar{L} = \bar{E}_k - \bar{E}_p = \frac{\operatorname{Im}(\bar{P}_{\text{in}})}{2\omega}. \tag{12c}$$

Eqs. (12a) and (12b) show that the equivalence of power exchange and energy in steady state is related to the potential energy only. The simplified expression (1a) involving kinetic energy is not correct, in particular where the local field variables are concerned. Yet the use of the local kinetic energy to express the local power dissipation is fairly common. While one part of losses of a small portion of a vibrating structure could indeed be attributed to its motion and thus to its kinetic energy, such as losses due to sound radiation, it seems unphysical to link the internal losses to kinetic rather than potential energy.

The loss factor for typical structures is very small. However, this should not imply that the second term in the numerator of Eq. (12b) could be neglected as the imaginary part of input mechanical power could often be much larger than the real part. Close to resonant frequencies the imaginary part is small in comparison to the real part and consequently the kinetic and potential energies will become almost identical at resonance.

If the loss factor is not constant over the vibrating body, a simple modification of the integral equation (12) is readily applicable:

$$\bar{P}_{\text{in}} = 2\omega\left(\mathrm{j}\bar{L} + \int_V \eta e_p \mathrm{d}V\right). \tag{12d}$$

This shows that the product between the local loss factor and potential energy rather than global values of these two quantities is responsible for energy dissipation within the structure.

Eqs. (11) and (12) hold strictly at all frequencies. These equations are not of statistical nature, thus no additional frequency averaging is needed. Obtained by direct integration of fundamental elasticity relationships they do not rely on limitations of modal approach. The only assumption was that on material linearity and on dissipation which was taken in the form of an isotropic, frequency dependent, internal loss factor. This makes Eqs. (11) and (12a–d) applicable to finite as well as infinite systems, to stationary vibration as well as to wave fields.

3.2. Example 2: energy in the field of Rayleigh waves

To illustrate the basic energy relationship (11) applied to the case of wave propagation, a simple example will be considered: that of two Rayleigh waves travelling in opposite directions in a semi-infinite solid. The computation of energy density and intensity was done using a procedure outlined in Appendix C (Fig. 4).

The material constants chosen correspond to light concrete: shear modulus $G = 1.5\,\text{GPa}$, mass density $\rho = 1300\,\text{kg/m}^3$, Poisson's ratio $\upsilon = 0.25$ and loss factor $\eta = 1.5\%$. The amplitude of the wave travelling in a negative direction was taken as 80% of that travelling in a positive direction. The phase between two waves is 90° at the reference position which is the centre of the displayed area.

The displayed area represents a cross-section through the solid, perpendicular to the free surface (top) and parallel to wave travelling direction, Fig. 4. The size of this area is 2.5 m in length and 0.5 m in depth.

Fig. 5 shows the kinetic (top) and potential (bottom) energy densities across the section at 1000 Hz, computed using the formulae presented in Appendix C. The free surface is at the top boundary. One can see that the two energies are very unevenly distributed with respect to each other. The mismatch between the kinetic and potential energy densities seen in Fig. 5 is typical of these quantities. Thus kinetic energy cannot be used as an indicator of the locations of internal losses.

Fig. 6 shows the real and imaginary part of time-averaged complex intensity vector in the selected cross section. The net energy is seen to flow almost in parallel with the surface. The imaginary part of intensity field has a strong vertical component which is deviated in the direction of the surface only very close to it. This case demonstrates how difficult would it be to try to establish an intuitive link between the energy density and energy flow.

The intensity was computed using Eq. (B.6). Its divergence was then evaluated by applying numerical differentiation to the field quantities entering intensity formula (B.6), using the x and y increments equal one millionth of the wavelength of shear waves. This was done to guarantee a straightforward check of the established relationships between energy and energy flow.

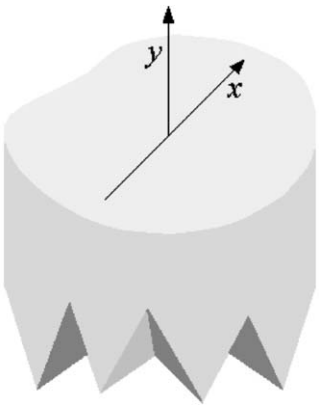

Fig. 4. Coordinate system used in the analysis of propagation of Rayleigh waves.

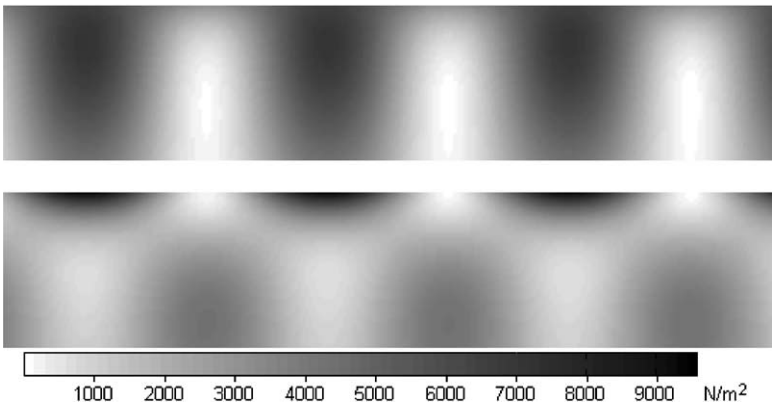

Fig. 5. Kinetic (top) and potential (bottom) time-averaged energy densities in the field of oppositely travelling Rayleigh waves. Material: light concrete, frequency: 1 kHz. Cross-section shown perpendicular to the free surface. Section area 2.5×0.5 m.

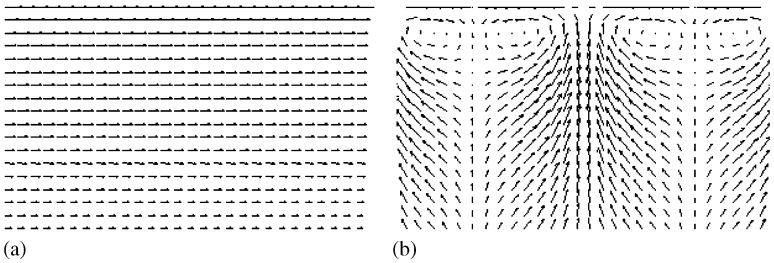

Fig. 6. (a) Real part and (b) imaginary part of complex intensity vector in the field of oppositely travelling Rayleigh waves in a semi-infinite solid. Same parameters as in Fig. 5. Section area 0.8×0.5 m corresponding to the leftmost position on Fig. 5.

Fig. 7 shows the real and imaginary parts of intensity divergence obtained by the numerical differentiation. With the actual value of loss factor, 1.5%, and the frequency of 1 kHz, the basic relationship (11) was shown to be perfectly valid.

The previous example clearly demonstrates that kinetic and potential energies can mutually be of very different values locally. Since potential energy is matched to net intensity divergence, this energy can serve as a reliable indicator of local energy loss distribution within a structure.

4. Non-uniform distribution of damping

The purpose of the next analysis is to investigate how an uneven distribution of damping within a system affects the relationships between the kinetic and potential energies and the input power to system (12a)–(12c). The analysis will be done on a linear system with lumped parameters as an uneven distribution of damping within such a system can easily be modelled analytically.

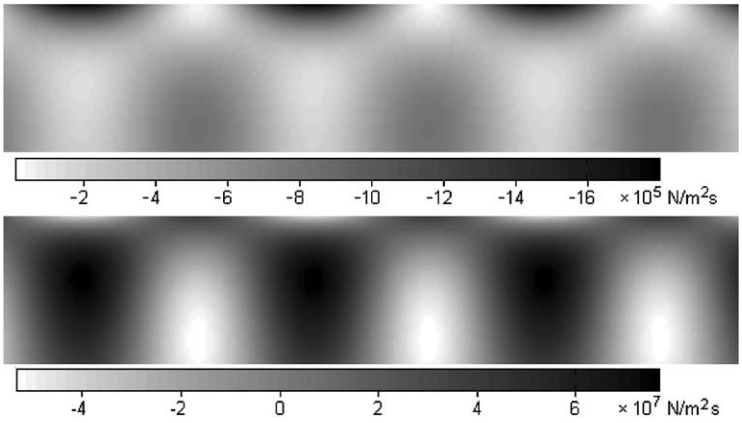

Fig. 7. Real part (top) and imaginary part (bottom) of complex intensity divergence in the field of oppositely travelling Rayleigh waves in a semi-infinite solid. Same parameters as in Fig. 5.

The system is analysed in Appendix D. It was shown that the global energy–power relationships hold providing the damping in the lumped dampers is proportional to the stiffness of the compliant elements. The damping can display an arbitrary frequency dependence but this dependence has to be the same for all dampers.

The principal advantage of the simple energy–power relationships (12b–d) is their independence of excitation. In cases where the damping satisfies the stiffness proportionality criterion, the three relationships, once established, will hold for any excitation. This is of particular value in all cases where the structure is excited at more than a single point.

In reality damping will rarely be uniformly distributed or stiffness proportional across a structure. It is worthwhile to find out how useful relationships (1), (1a) and (7) can be if applied to such a case. This will be illustrated through the next example.

4.1. Example 3: multi lumped parameter system with non-proportional damping

Consider a system consisting of 6 masses each of which possesses one. Each mass is connected to each other as well as to the ground by a hysteretically damped spring and a viscous dashpot. Each mass is excited by a force. The forces are of unequal amplitude and phase.

The mass and stiffness were chosen at random, using a random number generator. The mean values were then adjusted to 1 kg and 3×10^6 N/m, respectively. In this way the majority of resonant frequencies (five) entered the frequency range of analysis: 0–1 kHz. The excitation amplitudes and phases were equally chosen as random, between 0–1 N and 0–2π, respectively.

To start with, the damping was assumed to be zero. Fig. 8 shows the normalized difference between the kinetic and potential energies defined as the ratio of Lagrangian and total energy, hereby named for simplicity the "Lagrangian coefficient". Plot (a) shows the spread of this coefficient obtained by randomly varying the excitation forces 1000 times. It can be noticed that the Lagrangian coefficient of such a conservative system is zero at resonant frequencies. This was fully expected in accordance with the Rayleigh's principle.

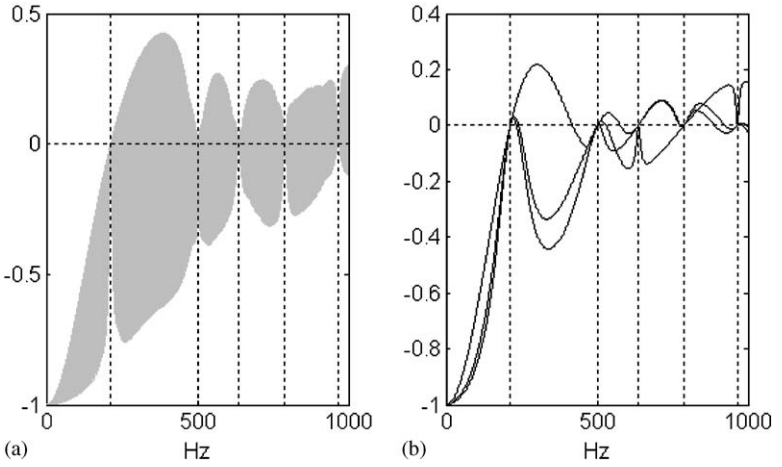

Fig. 8. Normalized difference of kinetic and potential energies in an undamped 6 dof system. (a) Spread of values obtained using 1000 different excitation conditions. (b) Case of 3 randomly chosen excitations. Vertical lines: resonant frequencies.

Plot (b) of Fig. 8 shows the Lagrangian coefficient for 3 distinct cases of excitation, chosen at random. It can be seen that the coefficient traverses each resonance at a positive slope, i.e. just below the resonance the potential energy is larger than the kinetic energy while the opposite applies just above the resonance. It follows that in-between any two resonances there exists a non-resonant frequency at which the two energies are equal. However, these off-resonant frequencies are not invariant of the system but depend on excitation distribution as clearly seen from Fig. 8b.

The presence of system damping changes the condition of equality of two energies: this occurs at frequencies shifted with respect to resonant frequencies. The shift is stronger the higher are the frequency and the damping.

In the following step the damping was adjusted to the proportionality criterion. The hysteretic loss factor was taken as 2% for all springs, while the damper rates of dashpots were made proportional to the corresponding spring stiffness. The viscous damping rate was chosen in such a way to give the same damping effect as the hysteretic damping when averaged over the analysed frequency band. This resulted in the average damper rate of 19.1 Ns/m.

As expected, Eqs. (12a) and (12b) were found to hold exactly at all frequencies.

The spring loss factors and the damper rate of dashpots were then randomly dispersed, still keeping the same mean values as in the previous case. Fig. 9 shows the total energy, $E_k + E_p$, and the Lagrangian energy, $E_k - E_p$. One can notice that close to resonances the difference of the two energies attains highest values in an absolute sense, but still lowest values in a relative sense.

To further examine the relationship between system energy and supplied power a global loss factor of the system had to be established. The simple half-power bandwidth technique was used for this purpose. Applied to the driving point mobility of the system, supposed accessible, this technique gives an estimate of the loss factor at resonance frequencies. By averaging over all input mobilities and by linearly fitting the results, the system's loss factor in the case considered was

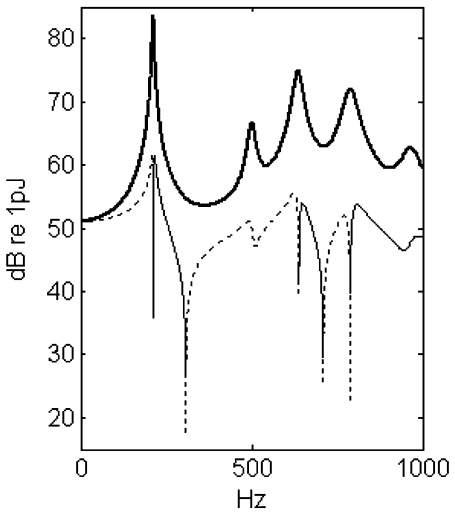

Fig. 9. Global energy of a non-proportionally damped 6 dof system. Thick: total energy, thin: positive values of Lagrangian energy, dashed: negative values of Lagrangian energy.

found to be equal to (the demonstration is straightforward and will thus be omitted):

$$\eta = 0.02 + 0.04f/1000$$

which matches well the selected values of the hysteretic and viscous damping.

Fig. 10 shows the dependence of the Lagrangian coefficient of the 6 dof system on damping at the upper part of frequency scale. To get a variation in damping the initial damping values were first increased by 2 and then by 5 times. The difference between the two energies is clearly increasing with the damping increasing. At higher frequencies and high damping the potential energy is always higher than the kinetic one.

With the fitted value of global loss factor, the potential and kinetic energies were estimated using Eq. (7), (12b) and (1a). Fig. 11 shows the results. The estimate of potential energy is reasonably good, being confined to an error between –20% and 2% throughout the frequency range. The estimate of kinetic energy via Eq. (12b) is of the same quality except at frequencies below the first resonance where the error attains unacceptably high values which increase with the frequency descending to zero. The estimate using Eq. (1a) gives unacceptable results even above the first resonance.

The error values in Fig. 11 apply also to an inverse case, that of estimating the loss factor via the potential energy and input power values. It should be noted that the exact value of system's loss factor is unknown, as this value is not prescribed in any obvious way but depends on the definition chosen. The matching between the estimate based on potential energy formulation (7) — thick curve, and the linearized estimate of loss factor defined previously can be considered as fairly good. The estimate which relies on kinetic energy, Eq. (1a) — thin full line, gives unacceptable results not only below the first resonance but at some higher frequencies as well. As such an estimate is used in the power injection method, e.g. [19], it could be worthwhile examining its accuracy.

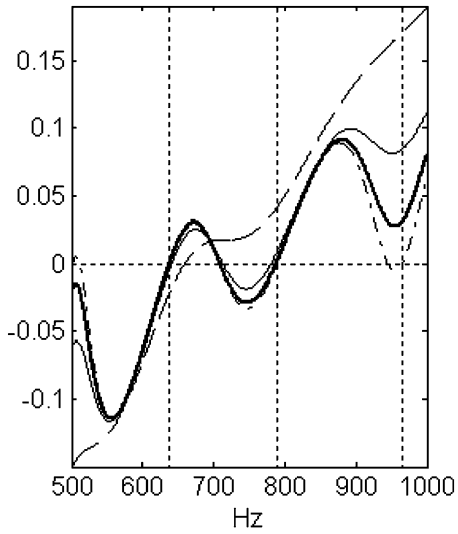

Fig. 10. Normalized difference of kinetic and potential energies in a 6 dof system in dependence of damping. Dash-dot line: no damping, thick line: rated damping; thin full line: rated damping $\times 2$; dashed line: rated damping $\times 5$. Vertical lines: resonant frequencies.

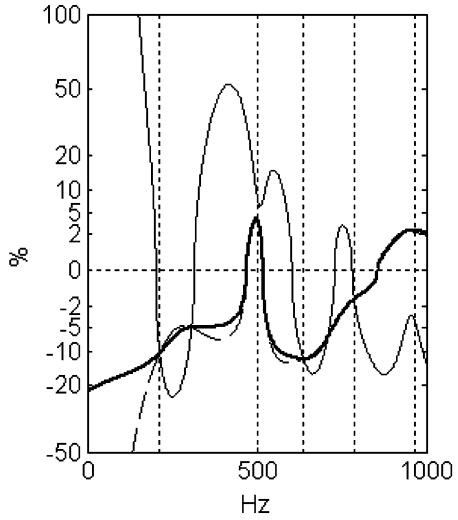

Fig. 11. Error in estimating the global energy of a non-proportionally damped 6 dof system using: thick line, potential energy, Eq. (7); full thin line, kinetic energy simplified, Eq. (1a); dashed line, kinetic energy, Eq. (12b). Vertical lines: resonant frequencies.

The differences in estimating loss factor by different formulations leads to a question about a convenient and robust definition of this quantity. Some comments on this subject are provided in the next section.

4.2. On the meaning of global loss factor in systems with non-homogeneous damping

Following the line of the previous example, an analysis will be made of the damping in the system with the objective to examine the definition of the global loss factor in this particular case.

The classical energy-based definition gives the loss factor as the ratio between the energy lost during one cycle of vibration and $2\pi \times$ the reversible mechanical energy. Eq. (11) follows this definition. While the energy formulation has a clear physical meaning where an elementary volume of solid matter is concerned, this meaning changes if the same formulation is applied to a global system exhibiting resonances.

Three energy definitions of loss factor were tested corresponding to Eqs. (1), (1a) and (7). The difference between the three is in the type of energy involved. The basic definition comprises the sum of kinetic and potential energies, Eq. (1), the "simple" definition replaces the total energy by twice the kinetic energy, Eq. (1a), and the present definition, based on (7), uses twice the potential energy instead.

The loss factor estimations by three definitions were repeated by 1000 consecutive computations, each with a different distribution of randomly generated excitation forces. Fig. 12 shows the result of the computation. Shown on the same diagram is the area of dispersion of loss factor estimates and the standard deviation of estimates normalized to the mean value.

It can be clearly seen that in the case of non-proportional damping, the loss factor estimate using the potential energy formulation, (7), gives much better results than the classical formulation which just vaguely indicates the correct trend of the global loss factor with frequency. The estimate via the kinetic energy is not only much inferior to the former two, but shows the frequency trend which is contrary to the true value.

In view of the established link between the net power input and the product loss factor — potential energy density, it could be argued that a "natural" definition of the global loss factor in

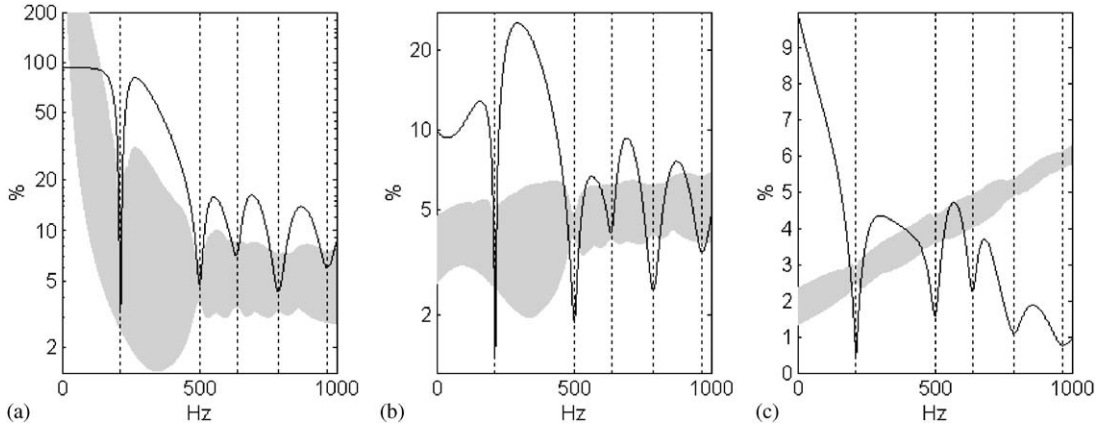

Fig. 12. 6 dof system: statistics of loss factor estimation based on 1000 randomly chosen force distributions. (a) Kinetic energy formulation, Eq. (1a); (b) classical definition, Eq. (1); (c) potential energy formulation, Eq. (7). Shaded area: estimation spread; solid line: normalized standard deviation of estimation. Vertical lines: resonant frequencies.

systems with an uneven damping distribution could be deduced from Eq. (12d):

$$\mathrm{Re}\{\bar{P}_{\mathrm{in}}\} = 2\omega \int_V \eta e_p \,\mathrm{d}V = 2\omega \eta_{\mathrm{global}} E_p \quad \Rightarrow \quad \eta_{\mathrm{global}} = \frac{\int_V \eta e_p \,\mathrm{d}V}{\int_V e_p \,\mathrm{d}V} = \frac{\mathrm{Re}\{\bar{P}_{\mathrm{in}}\}}{2\omega E_p}. \tag{13}$$

Defined in such a way, the global damping integrates conveniently the dissipation properties of a vibrating structure. However, while Eq. (13) is exact mathematically, it is of very modest practical importance: the global damping is not an intrinsic property of the structure but depends on the excitation as well. This is clearly demonstrated through the preceding examples.

Eq. (13) takes the distributed damping in an accurate way which in turn makes the global loss factor excitation-dependent. The conclusion is that the internal dissipation expressed via a global loss factor intrinsic to a given structure cannot be established, at least not in a unique way, unless the damping is homogeneously spread across the structure.

5. Conclusions

The energy flow can be linked to the system energy in a fairly straightforward way. Locally, the mean intensity divergence is proportional to the product of internal damping and potential energy density. If the intensity is represented in the complex form, the imaginary value of intensity divergence is proportional to the mean Lagrangian energy density at a given point.

On the global level, the temporal mean value of the total vibratory power input to a structure is proportional to the product between the loss factor and the global potential energy if the damping is isotropic and uniformly distributed within a structure. In such a case the global potential energy can be obtained from the known input power to the structure and the known loss factor. If the damping is not uniformly distributed but stays isotropic, an integral representation based on the product of the local loss factor and potential energy density is applicable, Eq. (12d). In this case the simple power – energy relationships, (1), (1a) and (7), are expected to hold approximately for potential energy but not necessarily for kinetic energy.

It has been concluded that the internal dissipation in a linear structure having the damping unevenly spread across it cannot be expressed via a unique, frequency-dependent global loss factor. Such a loss factor necessarily depends on the excitation and thus is not invariant of the structure itself.

The established proportionality between the net intensity divergence and the potential energy density can be used for an enhancement of experimental vibration analysis by

(1) Identifying "hot spots" within an elastic structure which, if locally damped, can be best suited for global vibration reduction. Such an identification can be done by measurement of potential energy distribution which is a task easier by far than any direct measurement of intensity divergence. This approach has been successfully checked by the author using computer simulations in the cases of vibrating beams and plates.
(2) Improving the robustness of energy flow measurement within a structure. Normally, the measurement of vibration intensity fails close to sources or discontinuities. The quantities needed to compute vibration intensity from measurement data are sufficient to compute the

potential energy density as well. The latter can be converted into intensity divergence which can be used in turn to check and rectify the obtained intensity maps.

Appendix A. Global energy and power using modal approach

According to Eq. (2a), the mean square velocity in a point x reads

$$\overline{\left|\dot{u}(x,\omega)\right|^2} = \frac{\omega^2}{2}\sum_q \sum_{q'} U_q U_{q'}^* \phi_q(x)\phi_{q'}(x). \tag{A.1}$$

The kinetic energy of the system is half the volume integral of the mean square velocity weighted by the mass density

$$\bar{E}_k = \frac{1}{2}\int_V \rho(x)\overline{\left|\dot{u}(x,\omega)\right|^2}\,\mathrm{d}V. \tag{A.2}$$

By inserting Eq. (A.1) into Eq. (A.2) and reverting the order of summation and integration one gets

$$E_k = \frac{\omega^2}{4}\sum_q \sum_{q'} U_q U_{q'}^* \int_V \rho(x)\phi_q(x)\phi_{q'}(x)\,\mathrm{d}V. \tag{A.3}$$

Since ϕ_q are normalized eigenfunctions, the integral in the expression above divided by the mass m becomes equal to Kronecker's operator in view of modal orthogonality. The kinetic energy thus becomes equal to a single modal sum

$$\bar{E}_k = \frac{m\omega^2}{4}\sum_q \left|U_q\right|^2. \tag{A.4}$$

The active input power is the sum of the product of external forces and the corresponding velocities

$$\bar{P} = \tfrac{1}{2}\mathrm{Re}\left(\sum_n F_n(\omega)v_n(\omega)^*\right). \tag{A.5}$$

Upon expressing the velocity by its modal sum, Eq. (2a), applied to the excitation positions z_n and changing the order of summation in Eq. (A.5) the following is obtained with the help of Eq. (2b)

$$\bar{P} = \frac{\omega}{2}\mathrm{Re}\left(\sum_q U_q^* \sum_n F_n(\omega)\phi_q(z_n)\right).$$

By rearranging the complex terms, the final expression for the time-averaged power assumes the following form:

$$\bar{P} = \frac{m\omega}{2}\sum_q \eta_q \omega_q^2 \left|U_q\right|^2. \tag{A.6}$$

The local value of the net power within the vibrating body, the intensity, can be assessed using modal summation too. The intensity is a vectorial quantity. Each component of intensity vector will be given as a sum of terms, each term being a product of a stress and a velocity component, (B.1). The stress itself is a function of displacement derivatives and involves elastic constant(s). Thus each term of each net intensity component can be represented as

$$I = -\tfrac{1}{2}\mathrm{Re}\{D\Theta[u(x,\omega)][\mathrm{j}\omega u(x,\omega)]^*\} = \frac{\omega}{2m^2}\mathrm{Re}\left\{D\sum_q\sum_{q'} U_q U_{q'}^* \Theta\left[\phi_q(x)\right]\phi_{q'}(x)\right\} \tag{A.7}$$

with $D = D_0(1+\mathrm{j}\eta)$ being the corresponding elasticity modulus and Θ a differential operator which relates the stress to the displacement.

Contrary to the expressions for global energy and power input, formula (A.7) cannot be reduced to a single modal sum. It can be further rearranged to show the influence of damping to local energy flow more explicitely:

$$I = \frac{\omega D}{2m^2}\sum_q\sum_{q'}\Theta(\phi_q)\phi_{q'}\left[\eta\mathrm{Re}(f_q f_{q'}^*)(\alpha_{qq'}+\beta_{qq'}) + \mathrm{Im}(f_q f_{q'}^*)(\alpha_{qq'}-\eta\beta_{qq'})\right],$$

$$\begin{aligned}\alpha_{qq'} &= \frac{(\omega_q^2-\omega^2)(\omega_{q'}^2-\omega^2)+\eta\omega_q^2\omega_{q'}^2}{[(\omega_q^2-\omega^2)^2+\eta^2\omega_q^4][(\omega_{q'}^2-\omega^2)^2+\eta^2\omega_{q'}^4]},\\ \beta_{qq'} &= \frac{\omega^2(\omega_q^2-\omega_{q'}^2)}{[(\omega_q^2-\omega^2)^2+\eta^2\omega_q^4][(\omega_{q'}^2-\omega^2)^2+\eta^2\omega_{q'}^4]}.\end{aligned} \tag{A.8}$$

The damping in a mechanical system thus produces an inter-modal coupling in the local energy flow. The nature of Eq. (A.8) is fairly complex as the stress function Θ cannot be universally reduced to modal parameters. As the coefficient α and the real part of modal force product are even functions with respect to the modal indices q and q' while the coefficient β and the imaginary part of modal force product are odd functions

$$\alpha_{qq'} = \alpha_{q'q}, \quad \mathrm{Re}(f_q f_{q'}^*) = \mathrm{Re}(f_{q'} f_q^*), \quad \beta_{qq'} = -\beta_{q'q}\mathrm{Im}(f_q f_{q'}^*) = -\mathrm{Im}(f_{q'} f_q^*)$$

Eq. (A.8) could be further simplified if the product $\Theta(\phi_q)\phi_q$ was itself either an even function or an odd one. This will depend on the case considered.

It should be noted that in the absence of damping the net intensity assumes a simple modal form

$$I = \frac{\omega D}{2m^2}\sum_q\sum_{q'}\frac{\Theta(\phi_q)\phi_{q'}\mathrm{Im}(f_q f_{q'}^*)}{(\omega_q^2-\omega^2)(\omega_{q'}^2-\omega^2)}. \tag{A.8a}$$

The last expression shows that the energy flow will exist even if the structure is lossless. If however the excitations are in phase or 180° out of phase there will be no flow of energy in such a structure.

Appendix B. Energy density, intensity and intensity divergence

Assume for simplicity Cartesian coordinates. At a particular point the vibration displacement can be represented by its x,y,z components

$$\mathbf{u} = u_x\mathbf{i} + u_y\mathbf{j} + u_z\mathbf{k}.$$

The strains are spatial derivatives of displacements. Shown below are the relationships only for x-direction: analogous expressions are valid for y and z directions through subscript permutation

$$\varepsilon_{xx} = \frac{\partial u_x}{\partial x},\ \varepsilon_{yy} = \cdots,\ \varepsilon_{zz} = \cdots,\ \varepsilon_{xy} = \varepsilon_{yx} = \frac{\partial u_x}{\partial y} + \frac{\partial u_y}{\partial x},\ \varepsilon_{yz} = \varepsilon_{zy} = \cdots,\ \varepsilon_{zx} = \varepsilon_{xz} = \cdots \quad \text{(B.1)}$$

Equation of motion (equally shown for x-direction only)

$$\frac{\partial \sigma_{xx}}{\partial x} + \frac{\partial \sigma_{xy}}{\partial y} + \frac{\partial \sigma_{xz}}{\partial z} = \rho \ddot{u}_x. \quad \text{(B.2)}$$

The instantaneous kinetic and potential energy densities read

$$e_k = \tfrac{1}{2}\rho\left(\dot{u}_x^2 + \dot{u}_y^2 + \dot{u}_z^2\right), \quad \text{(B.3)}$$

$$e_p = \tfrac{1}{2}(\sigma_{xx}\varepsilon_{xx} + \sigma_{yy}\varepsilon_{yy} + \sigma_{zz}\varepsilon_{zz} + \sigma_{xy}\varepsilon_{xy} + \sigma_{yz}\varepsilon_{yz} + \sigma_{zx}\varepsilon_{zx}). \quad \text{(B.4)}$$

The intensity vector can be represented by its orthogonal x,y,z components

$$\mathbf{I} = I_x\mathbf{i} + I_y\mathbf{j} + I_z\mathbf{k}. \quad \text{(B.5)}$$

The intensity component in x direction reads

$$I_x = -(\sigma_{xx}\dot{u}_x + \sigma_{xy}\dot{u}_y + \sigma_{xz}\dot{u}_z) \quad \text{(B.6)}$$

with the negative sign taken to represent the sense of energy flow in a correct physical way. The intensity divergence is

$$\nabla \cdot \mathbf{I} = \frac{\partial I_x}{\partial x} + \frac{\partial I_y}{\partial y} + \frac{\partial I_z}{\partial z}. \quad \text{(B.7)}$$

By carrying out the differentiation in Eq. (B.7) and making use of equation of motion (B.2) as well as of strain–displacement formulae (B.1) the following is obtained for intensity divergence:

$$\nabla \cdot \mathbf{I} = -\left[\rho(\ddot{u}_x\dot{u}_x + \ddot{u}_y\dot{u}_y + \ddot{u}_z\dot{u}_z) + \sigma_{xx}\dot{\varepsilon}_{xx} + \sigma_{yy}\dot{\varepsilon}_{yy} + \sigma_{zz}\dot{\varepsilon}_{zz} + \sigma_{xy}\dot{\varepsilon}_{xy} + \sigma_{yz}\dot{\varepsilon}_{yz} + \sigma_{zx}\dot{\varepsilon}_{zx}\right]. \quad \text{(B.8)}$$

Eqs. (B.1)–(B.8) represent instantaneous values of field quantities. The only assumption made so far is that of material linearity. To simplify further steps material will be assumed homogeneous and isotropic. Generalised Hooke's law then yields simple stress–strain relationships

$$\sigma_{xx} = (\lambda_0 + 2\mu_0)\varepsilon_{xx} + \lambda_0(\varepsilon_{yy} + \varepsilon_{zz}), \quad \sigma_{xy} = \mu_0\varepsilon_{xy}, \quad \sigma_{xz} = \mu_0\varepsilon_{xz}, \quad \text{(B.9)}$$

where λ_0 and μ_0 are Lamé's constants of lossless material.

The Hooke's law characterizing a linear elastic solid provides linear relationships between strains and stresses. In a dissipative solid exhibiting vibration the instantaneous stresses and strains are not proportional. In order to keep the proportionality, harmonic time variations with frequency ω are assumed. The proportionality between strains and stresses is then applied to

amplitudes, not to instantaneous values. All the varying quantities can then be represented as complex. In addition, the elasticity constants have to be made complex too to take the dissipation into account:

$$\lambda = \lambda_0(1 + \mathrm{j}\eta), \quad \mu = \mu_0(1 + \mathrm{j}\eta) \tag{B.10}$$

Using Eq. (B.9) in complex form, different products in (B.4) can be expressed in terms of complex strain amplitudes and grouped in the following way:

$$\sigma_{xx}\varepsilon_{xx} + \sigma_{yy}\varepsilon_{yy} + \sigma_{zz}\varepsilon_{zz} = (\lambda/2 + \mu)\Gamma_1 + \lambda\Gamma_2, \quad \sigma_{xy}\varepsilon_{xy} + \sigma_{yz}\varepsilon_{yz} + \sigma_{zx}\varepsilon_{zx} = \mu/2\Gamma_3,$$
$$\Gamma_1 = \left|\Xi_{xx}^2\right| + \left|\Xi_{yy}^2\right| + \left|\Xi_{zz}^2\right|, \quad \Gamma_2 = \mathrm{Re}(\Xi_{xx}\Xi_{yy}^* + \Xi_{yy}\Xi_{zz}^* + \Xi_{zz}\Xi_{xx}^*), \quad \Gamma_3 = \left|\Xi_{xy}^2\right| + \left|\Xi_{yz}^2\right| + \left|\Xi_{zx}^2\right|, \tag{B.11}$$

where the symbol Ξ stands for complex strain amplitude. Note that all Γ terms are real.

The time-averaged potential energy density corresponds to the real part of amplitude products involved, thus

$$\bar{e}_p = \tfrac{1}{2}\left[(\lambda_0/2 + \mu_0)\Gamma_1 + \lambda_0\Gamma_2 + \mu_0/2\Gamma_3\right]. \tag{B.12}$$

The time averaged kinetic energy is obtained from Eq. (B.3) in terms of displacement amplitude squares

$$\bar{e}_k = \frac{\omega^2}{4}\left[\left|U_x^2\right| + \left|U_y^2\right| + \left|U_z^2\right|\right]. \tag{B.13}$$

By expressing the time-averaged intensity divergence in complex form, comprising the substitution of time derivatives by $\mathrm{j}\omega$ multiplication, and by applying Eq. (B.11) the complex form of intensity divergence is obtained from Eq. (B.8) as

$$\nabla \cdot \mathbf{I} = -\mathrm{j}\omega^3\left(\left|U_x^2\right| + \left|U_y^2\right| + \left|U_z^2\right|\right)\Big/2 + \mathrm{j}\omega\left[(\lambda/2 + \mu)\Gamma_1 + \lambda\Gamma_2 + \mu/2\Gamma_3\right]. \tag{B.14}$$

Splitting Eq. (B.14) into its real and imaginary parts yields

$$\mathrm{Re}(\nabla \cdot \mathbf{I}) = -\eta\omega\left[(\lambda_0/2 + \mu_0)\Gamma_1 + \lambda_0\Gamma_2 + \mu_0/2\Gamma_3\right],$$
$$\mathrm{Im}(\nabla \cdot \mathbf{I}) = -\omega^3\left(\left|U_x^2\right| + \left|U_y^2\right| + \left|U_z^2\right|\right)\Big/2 + \omega\left[(\lambda_0/2 + \mu_0)\Gamma_1 + \lambda_0\Gamma_2 + \mu_0/2\Gamma_3\right]. \tag{B.15}$$

By comparing Eqs. (B.15) with (B.12) and (B.13) it can be seen that the complex intensity divergence fully determines the energy density within an elastic vibrating object

$$\mathrm{Re}(\nabla \cdot \mathbf{I}) = -2\eta\omega\bar{e}_p, \tag{B.16a}$$

$$\mathrm{Im}(\nabla \cdot \mathbf{I}) = -2\omega(\bar{e}_k - \bar{e}_p) = -2\omega\bar{\ell} \tag{B.16b}$$

ℓ being the Lagrangian density, $\ell = e_k - e_p$.

The last two equations represent a fundamental relationship between energy and energy flow in an elastic structure. The assumptions used are quite weak: the material should be linear while the internal energy dissipation should match the concept of complex loss factor. It should be pointed out that no assumption was made as to the frequency dependence of loss factor. In particular, the loss factor does not have to be frequency independent. It can obey any frequency dependence, but

has to be the same for the entire structure and for all kind of deformations. The condition of material isotropy and homogeneity is not essential and can be removed at a cost of resorting to relationships used in physics of solids.

The divergence–energy relationship (B.16) was obtained using Eq. (B.2) which applies to zones free from external excitation. The net divergence is seen to be always negative. The result is thus physically clear: in excitation-free areas the power is always lost by dissipation.

Appendix C. Energy density and intensity of a surface wave field

Let the position of the x–z plane of a Cartesian coordinate system coincide with the free surface of a semi-infinite solid. The wave propagation is chosen such to take place along the x-axis, Fig. 4. Two surface (Rayleigh) waves of unequal amplitudes are supposed to travel in the opposite directions.

The wave field variables can be derived from two functions: one velocity potential Φ and one stream function ψ, [20]. The first represents dilatational waves travelling at the speed c_d, the second one represents shear waves travelling at the speed c_s:

$$c_s = \sqrt{\frac{G}{\rho}}, \quad c_d = \sqrt{\frac{\lambda + 2\mu}{\rho}} = c_s\sqrt{\frac{2(1-\upsilon)}{1-2\upsilon}}. \tag{C.1}$$

A harmonic positive propagating wave will be represented by the following pair (exponential time factor omitted):

$$\Phi = A_\Phi \mathrm{e}^{-\mathrm{j}sx+qy}, \quad \Psi = A_\Psi \mathrm{e}^{-\mathrm{j}sx+gy}. \tag{C.2}$$

Here s stands for the wavenumber projection in the x-axis which has to be the same for both the dilatational and shear waves. The wavenumber projection in y direction is necessarily imaginary for both waves, meaning that the motion from the surface will decay exponentially in the depth. The wavenumber triangle rule has to be satisfied, giving the (real) values of q and g:

$$q = \sqrt{s^2 - \omega^2/c_d^2}, \quad g = \sqrt{s^2 - \omega^2/c_s^2} \tag{C.3}$$

since $s > \omega/c_s > \omega/c_d$. The character of surface waves imposes constraints on the wave motions, which results in an equation giving s as its real root:

$$4s^2\sqrt{(s^2 - \omega^2/c_d^2)(s^2 - \omega^2/c_s^2)} = (\omega^2/c_s^2 - 2s^2)^2. \tag{C.4}$$

Finally, the amplitudes of Φ and Ψ functions cannot be independent, but have to satisfy the next compatibility condition:

$$\frac{A_\Psi}{A_\Phi} = \mathrm{j}\frac{2s\sqrt{s^2 - \omega^2/c_d^2}}{2s^2 - \omega^2/c_s^2} = X. \tag{C.5}$$

Given one of the two amplitudes, both functions Φ and Ψ, and thus the whole field, become fully defined via Eqs. (C.1)–(C.5). The x and y components of particle velocity of the Rayleigh wave

read, [20]

$$\dot{u}_x = \frac{\partial \Phi}{\partial x} + \frac{\partial \Psi}{\partial y}, \quad \dot{u}_y = \frac{\partial \Phi}{\partial y} - \frac{\partial \Psi}{\partial x}. \tag{C.6}$$

The formula (C.6) holds for a wave travelling in the direction of positive x axis. A wave moving in the negative direction must have the x velocity component of the opposite sign while its y velocity component has to be the same as for the positive wave. These two conditions allow the construction of the total field, i.e. the sum of two waves in the following way:

$$\begin{aligned} \Phi &= A_{\Phi+}\mathrm{e}^{-\mathrm{j}sx+qy} + A_{\Phi-}\mathrm{e}^{\mathrm{j}sx+qy} = \Phi_+ + \Phi_-, \\ \Psi &= A_{\Psi+}\mathrm{e}^{-\mathrm{j}sx+gy} + A_{\Psi-}\mathrm{e}^{\mathrm{j}sx+gy} = X(A_{\Phi+}\mathrm{e}^{-\mathrm{j}sx+gy} - A_{\Phi-}\mathrm{e}^{\mathrm{j}sx+gy}) = \Psi_+ - \Psi_-. \end{aligned} \tag{C.7}$$

The complex amplitudes of particle displacements and strains can be now readily evaluated

$$\begin{aligned} U_x &= \frac{1}{\mathrm{j}\omega}[-\mathrm{j}s(\Phi_+ - \Phi_-) + g(\Psi_+ - \Psi_-)], \\ U_y &= \frac{1}{\mathrm{j}\omega}[q(\Phi_+ + \Phi_-) + \mathrm{j}s(\Psi_+ + \Psi_-)], \\ \Xi_{xx} &= \frac{1}{\mathrm{j}\omega}\left[-s^2(\Phi_+ + \Phi_-) - \mathrm{j}s\, g(\Psi_+ + \Psi_-)\right], \\ \Xi_{yy} &= \frac{1}{\mathrm{j}\omega}\left[q^2(\Phi_+ + \Phi_-) + \mathrm{j}s\, g(\Psi_+ + \Psi_-)\right], \\ \Xi_{xy} &= \frac{1}{\mathrm{j}\omega}\left[-2\mathrm{j}s\, q(\Phi_+ - \Phi_-) + (s^2 + g^2)(\Psi_+ - \Psi_-)\right]. \end{aligned} \tag{C.8}$$

The stresses can be computed from the known strains using Eq. (B.9) and setting z-dependent terms to zero. To allow for the damping in the material, the elasticity constants have to be made complex. According to Eq. (C.1) this will yield velocities of dilatational and shear waves complex too, and consequently all the expressions Eqs. (C.3)–(C.5) have to be adjusted for complex c_d, c_s, s, q and g.

Finally, the kinetic and potential energy densities can be computed using Eqs. (B.13) and (B.12), while the intensity follows from Eq. (B.6) applying the complex elastic constants.

Appendix D. Energy and power in a lumped-parameter system

The energy analysis of a multi-dof system with lumped parameters can be done by considering a 2 dof system first. The results can be then easily generalized.

Fig. 13 shows a linear 2 dof system. Each of the two masses is grounded via a spring and a dashpot. The two masses are also linked mutually via a spring and a dashpot.

The damping force in the dashpot is supposed to be linearly related to the relative displacements of the two ends:

$$F_{\mathrm{damp}} = \mathrm{j}\gamma\, u_{\mathrm{rel}}, \quad \gamma = \gamma(\omega). \tag{D.1}$$

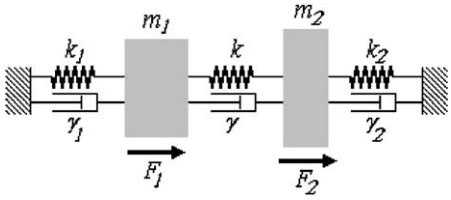

Fig. 13. 2 dof system.

By allowing an arbitrary frequency dependence of the damping function γ, any type of linear damping can be taken into account. For example, hysteretic damping is obtained by setting $\gamma = k\eta$ while viscous damping corresponds to $\gamma = c\omega$ with k and η denoting the stiffness and loss factor of the associated spring while c stands for viscous damper rate. A viscous dashpot in parallel with a hysteretically damped spring will give the damping function $\gamma = k\eta + c\omega$.

The damping functions of the three dampers are assumed to be mutually different. The following expressions can be obtained for the kinetic energy, potential energy, net input power and imaginary input power:

$$
\begin{aligned}
E_k &= \frac{1}{4|D|^2}\left[\varsigma_1|F_1^2| + \varsigma_2|F_2^2| + 2\varsigma_r \mathrm{Re}\{F_1F_2^*\} + 2\varsigma_i \mathrm{Im}\{F_1F_2^*\}\right],\\
E_p &= \frac{1}{4|D|^2}\left[\xi_1|F_1^2| + \xi_2|F_2^2| + 2\xi_r \mathrm{Re}\{F_1F_2^*\} + 2\xi_i \mathrm{Im}\{F_1F_2^*\}\right],\\
\mathrm{Re}\{\mathbf{P}_{in}\} &= \frac{\omega}{2|D|^2}\left[\beta_{r1}|F_1^2| + \beta_{r2}|F_2^2| + 2\beta_r \mathrm{Re}\{F_1F_2^*\}\right],\\
\mathrm{Im}\{\mathbf{P}_{in}\} &= \frac{\omega}{2|D|^2}\left[\beta_{i1}|F_1^2| + \beta_{i2}|F_2^2| + 2\beta_i \mathrm{Re}\{F_1F_2^*\}\right],\\
D &= (\lambda_1 + \mathrm{j}\gamma_1)(\lambda_2 + \mathrm{j}\gamma_2) + (k + \mathrm{j}\gamma)[\lambda_1 + \lambda_2 + \mathrm{j}(\gamma_1 + \gamma_2)].
\end{aligned}
\tag{D.2}
$$

Using the abbreviation $\lambda = k - \omega^2 m$ after some tedious exercise the coefficients of Eq. (D.2) can be found as

$$
\begin{aligned}
\varsigma_1 &= m_1\omega^2\left[(\lambda_2 + k)^2 + (\gamma_2 + \gamma)^2\right] + m_2\omega^2(k^2 + \gamma^2),\\
\varsigma_2 &= m_2\omega^2\left[(\lambda_1 + k)^2 + (\gamma_1 + \gamma)^2\right] + m_1\omega^2(k^2 + \gamma^2),\\
\varsigma_r &= m_1\omega^2(\lambda_2 k + \gamma_2\gamma) + m_2\omega^2(\lambda_1 k + \gamma_1\gamma) + (m_1 + m_2)\omega^2(k^2 + \gamma^2),\\
\varsigma_i &= m_1\omega^2(\gamma_2 k + \lambda_2\gamma) - m_2\omega^2(\gamma_1 k + \lambda_1\gamma),
\end{aligned}
\tag{D.2a}
$$

$$
\begin{aligned}
\xi_1 &= k_1\left[(\lambda_2 + k)^2 + (\gamma_2 + \gamma)^2\right] + k_2(k^2 + \gamma^2) + k(\lambda_2^2 + \gamma_2^2),\\
\xi_2 &= k_2\left[(\lambda_1 + k)^2 + (\gamma_1 + \gamma)^2\right] + k_1(k^2 + \gamma^2) + k(\lambda_1^2 + \gamma_1^2),\\
\xi_r &= k(k_1k_2 - m_1m_2\omega^4 - \gamma_1\gamma_2) + \gamma(k_1\gamma_2 + k_2\gamma_1) + (k_1 + k_2)(k^2 + \gamma^2),\\
\xi_i &= \omega^2\left[k(m_1\gamma_2 - m_2\gamma_1) - \gamma(m_1k_2 - m_2k_1)\right],
\end{aligned}
\tag{D.2b}
$$

$$\begin{aligned}\beta_{r1} &= \gamma_1\left[(\lambda_2+k)^2+(\gamma_2+\gamma)^2\right]+\gamma_2(k^2+\gamma^2)+\gamma(\lambda_2^2+\gamma_2^2),\\ \beta_{r2} &= \gamma_2\left[(\lambda_1+k)^2+(\gamma_1+\gamma)^2\right]+\gamma_1(k^2+\gamma^2)+\gamma(\lambda_1^2+\gamma_1^2),\\ \beta_r &= k(\lambda_1\gamma_2+\lambda_2\gamma_1)-\gamma(\lambda_1\lambda_2-\gamma_1\gamma_2)+(\gamma_1+\gamma_2)(k^2+\gamma^2),\end{aligned} \tag{D.2c}$$

$$\begin{aligned}\beta_{i1} &= -\lambda_1\left[(\lambda_2+k)^2+(\gamma_2+\gamma)^2\right]-\lambda_2(k^2+\gamma^2)-k(\lambda_2^2+\gamma_2^2),\\ \beta_{i2} &= -\lambda_2\left[(\lambda_1+k)^2+(\gamma_1+\gamma)^2\right]-\lambda_1(k^2+\gamma^2)-k(\lambda_1^2+\gamma_1^2),\\ \beta_i &= -\gamma(\lambda_1\gamma_2+\lambda_2\gamma_1)-k(\lambda_1\lambda_2-\gamma_1\gamma_2)-(\lambda_1+\lambda_2)(k^2+\gamma^2).\end{aligned} \tag{D.2d}$$

An expression analogous to Eq. (D.2) would apply to a system having more degrees of freedom than 2, only the number of terms would be larger. For an N dof system, there would be N direct terms and $N(N-1)/2$ cross-terms. The coefficients (D.2a)–(D.2d) would be exactly the same. Thus the present analysis can be considered as being universally applicable to all linear lumped-parameter systems.

By comparing coefficients (D.2a), (D.2b) and (D.2d) the following equalities can be established:

$$\varsigma_1-\xi_1=\beta_{i1},\quad \varsigma_2-\xi_2=\beta_{i2},\quad \varsigma_r-\xi_r=\beta_i,\quad \varsigma_i-\xi_i=0. \tag{D.3}$$

When inserted into Eq. (D.2) these equalities confirm the validity of the relationship between the total Lagrangian energy of the system and the imaginary part of input power to it, (9.d). This relationship is valid as long as the system is linear, no matter what is the nature of damping and how is the damping is distributed within the system.

By looking at Eq. (D.2), it can be seen that the expressions for the kinetic and potential energies contain a term involving the imaginary part of the product between the excitation forces. The input power does not depend on this product, yet the imaginary input power is strictly proportional to the difference of two energies. The reason for this apparent inconsistency becomes obvious when the coefficients ς_i and ξ_i which multiply the imaginary power term are examined more closely: the two are equal, thus making their difference vanish, see Eq. (D.3).

Regretfully, the relationship between the potential energy of the system and the active input power cannot be obtained for any arbitrary linear damping. In particular, the contribution of the imaginary power term appearing in the expression for potential energy is not compensated for in this case and will thus produce already on its own a source of unbalance between the coefficients of potential energy and active power. Other corresponding coefficients will not be identical either, thus the equality between the potential energy and the weighted net input power will not hold in the case of arbitrary system damping.

Formally, the damping function γ of any spring–dashpot pair, as defined by Eq. (D.1), can be represented as a product of a non-dimensional coefficient η and the spring stiffness. In a general linear case η will be frequency dependent and different for each spring-dashpot, see (D.1):

$$\gamma_i=\eta_i(\omega)k_i. \tag{D.1a}$$

Now, if the coefficient $\eta(\omega)$ is the same for each spring-dashpot pair

$$\gamma_i=\eta(\omega)k_i \tag{D.4}$$

the corresponding coefficients in the expressions for potential energy, ξ, and net input power, β_r, become strictly identical, while the non-compensated coefficient ξ_i becomes zero

$$\xi_1 = \beta_{r1}, \quad \xi_2 = \beta_{r2}, \quad \xi_r = \beta_r, \quad \xi_i = 0. \tag{D.5}$$

In this case, clearly, the simple relationship between the potential energy and the net input power, (12a), becomes valid.

The proportionality between the damping function γ and the spring rate k, which expresses the concept of 'proportional damping' is often used in numerical modal analysis where it is needed to apply the eigenvalue solution to damped systems. It should be noted that Eq. (D.4) does not reduce the coefficient η to the role of constant loss factor, but allows for an arbitrary frequency dependence of this coefficient.

References

[1] R.H. Lyon, R.G. de Jong, *Theory and Application of Statistical Energy Analysis*, Second ed., Butterworth-Heinemann, Boston, 1995.

[2] D. Karnopp, Coupled vibratory system analysis using the dual formulation, *Journal of the Acoustical Society of America* 2 (1966) 380–384.

[3] R.S. Langley, A general derivation of the statistical energy analysis equations for coupled dynamic systems, *Journal of Sound and Vibration* 135 (1989) 499–508.

[4] L. Gavric, G. Pavic, A finite element method for computation of structural intensity by the normal mode approach, *Journal of Sound and Vibration* 164 (1993) 29–43.

[5] V.D. Belov, S.A. Rybak, B.D. Tartakovskii, Propagation of vibrational energy in absorbing structures, *Soviet Physics Acoustics* 23 (1977) 115–119.

[6] D.J. Nefske, S.H. Sung, Power flow finite element analysis of dynamic systems: theory and application to beams, *Journal of Vibration, Acoustics, Stress and Reliability in Design* 111 (1989) 94–100.

[7] J.C. Wohlever, R.J. Bernhard, Mechanical energy flow models of rods and beams, *Journal of Sound and Vibration* 153 (1992) 1–19.

[8] M. Djimadoum, J-L. Guyader, Vibratory prediction with an equation of diffusion, *Acta Acustica* 3 (1995) 11–24.

[9] A. Carcaterra, A. Sestieri, Energy density equations and power flow in structures, *Journal of Sound and Vibration* 188 (1995) 269–282.

[10] W. Maysenhölder, *Energy of Structure-borne Sound*, S. Hirzel Verlag, Stuttgart, 1994 (in German).

[11] B.A. Auld, Second ed, *Acoustic Fields and Waves in Solids*, Vol. 1, Krieger Publishing, Malabar, 1990.

[12] K.S. Alfredsson, Active and reactive structural energy flow, *Journal of Vibration and Acoustics* 119 (1997) 70–79.

[13] E. Skudrzyk, *Simple and Complex Vibratory Systems*, The Pennsylvania State University Press, University Park, 1968.

[14] G.B. Warburton, *The Dynamical Behaviour of Structures*, Second ed., Pergamon, Oxford, 1976.

[15] Yu.I. Bobrovnitskii, Some energy relations for mechanical systems, in: F.J. Fahy, W.G. Price (Eds.), *IUTAM Symposium on Statistical Energy Analysis*, Kluwer, Dordrecht, 1999, pp. 37–46.

[16] Yu.I. Bobrovnitskii, Estimating the vibrational energy characteristics of an elastic structure via the input impedance and mobility, *Journal of Sound and Vibration* 217 (1998) 351–386.

[17] Yu.I. Bobrovnitskii, M.P. Korotkov, Improved estimates for the energy characteristics of a vibrating elastic structure via the input impedance and mobility: experimental verification, *Journal of Sound and Vibration* 247 (2001) 683–702.

[18] L. Cremer, M. Heckl, E.E. Ungar, *Structure-Borne Sound*, Springer, Berlin, 1988.

[19] D.A. Bies, S. Hamid, In situ determination of loss and coupling loss factors by the power injection method, *Journal of Sound and Vibration* 91 (1980) 187–204.

[20] K.F. Graff, *Elastic Waves in Solids*, Clarendon Press, London, 1975.